J Mol Model (2002) 8:231–236
DOI 10.1007/s00894-002-0091-z

ORIGINAL PAPER

**Antje Germer · Sabrina Klod · Martin G. Peter**
**Erich Kleinpeter**

# NMR spectroscopic and theoretical study of the complexation of the inhibitor allosamidin in the binding pocket of the plant chitinase hevamine

Received: 8 May 2002 / Accepted: 26 June 2002 / Published online: 1 August 2002


**Abstract** Based on NMR spectroscopic information about the allosamidin–hevamine complex, ab initio MO calculations of the ring current effect of the aromatic moieties of Trp255, Tyr183 and Tyr6 of hevamine were carried out to investigate the role of these amino acid residues in binding interactions with allosamidin in solution. In addition, the intermolecular steric compression effect on the $^{13}C$ chemical shifts of the allosamizoline carbon atoms and the hydrogen bonding to Glu127 was identified. It can be inferred that the binding forces are strongest in the allosamizoline moiety of allosamidin.

**Keywords** Allosamidin · Hevamine · NMR spectroscopy · Ab initio calculations · Ring current effect

## Introduction

Many plants infected with pathogens develop local or systemic resistance against subsequent infections. [1] The induction of this pathogen resistance proved to be correlated with the production of "pathogenesis-related" proteins. [2] However, subsequent investigations revealed that at least some of these pathogenesis-related proteins can also be found in healthy plants [3, 4] and are expressed constitutively. [5] The function of these proteins in plants seems to be to provide the plant with a general, unspecific defense against attack by microbial pathogens and insects. Therefore, these proteins and their inhibitors are of general interest.

Hevamine, [6] an enzyme with chitinase activity, can be isolated from fresh latex, obtained by tapping the rubber tree *Hevea brasiliensis*. Chitinases are enzymes that cleave the bond between two consecutive *N*-acetylglucosamines of chitin, a major component of the cell wall of many fungi and of the exoskeleton of insects.

Hevamine belongs to the family of 18 chitinases. The crystal structure was refined at 1.8 Å resolution and the reaction mechanism is theoretically quite well understood. [7, 8, 9, 10] In addition to the knowledge about the reaction mechanism, especially the binding features in aqueous solution are important for the design of new transition state analogues that may act as chitinase inhibitors and potential insecticides [11, 12] and/or fungicides. [13] It is the objective of this paper to report on the influence of the amino acids Trp255, Tyr183 and Tyr6 of the enzyme hevamine on the $^{1}H/^{13}C$ NMR spectra of the inhibitor allosamidin concerning binding interactions at the active site (Fig. 1). In order to do this, NMR spectroscopic structural information has been corroborated by ab initio quantum chemical calculations.

## Experimental

Hevamine was isolated from latex of *Hevea brasilienis* in the laboratory of J.J. Beintema, Laboratory of Biochemistry, Rijksuniversiteit Groningen, The Netherlands. Allosamidin was a generous gift from A. Isogai, Department of Agricultural Chemistry, University of Tokyo, Japan.

### NMR experiments

$^{1}H$ and $^{13}C$ NMR spectra were measured on a Bruker DMX 600 NMR spectrometer at 600 and 150 MHz, respectively. Sample tubes of 5 mm outer diameter were used and the NMR spectra recorded at 313 K without sample-spinning using the HDO signal as internal reference (4.61 ppm at 313 K). Data acquisition and processing were performed with X WIN-NMR software (BRUKER).

For the assignment of the $^{1}H$ and $^{13}C$ NMR spectra, H,H-COSY and phase-sensitive H,C-COSY (HMQC),

A. Germer · S. Klod · M.G. Peter · E. Kleinpeter (✉)
Universität Potsdam, Institut für Chemie, P.O. Box 601553,
14415 Potsdam, Germany
e-mail: kp@chem.uni-potsdam.de
Tel.: +49-331-977-5210/Secr. 5211
Fax: +49-331-977-5064/Secr. 5057

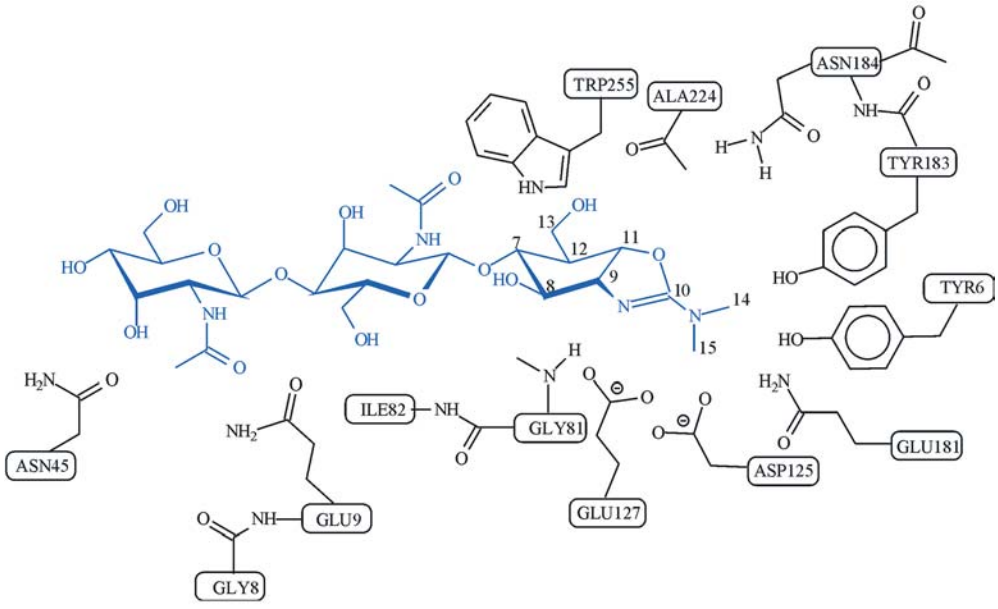


**Fig. 1** Schematic representation of the active site of the hevamine – allosamidin (*blue*-colored) complex [8]

H,C long range correlation (HMBC) as well as HMQC-TOCSY NMR experiments were performed.

Two-dimensional transfer NOESY (trNOESY) [14] experiments were recorded with a total of 512 ($t_1$)×2 K ($t_2$) data points for each experiment. The HDO signal was suppressed by low-power presaturation during the relaxation and mixing time. The total relaxation delay was 1.2 s. Mixing times of 150 ms, 300 ms and 600 ms were used.

For the 1D saturation transfer difference experiments (STD), [15] the saturation transfer was achieved by using 39 selective 1 K Gaussian 90° pulses with a duration of 50 ms and a spacing of 1 ms. For one set of NMR spectra, the protein envelope was irradiated at 1.2 ppm (on-resonance) and 20 ppm (off-resonance). Another set of spectra was generated by setting the on-resonance frequency to 7.2 ppm. Subsequent subtraction was achieved via phase cycling. Saturation times were 0.5, 1.0, 1.5 and 2 s. The relaxation delay was set to 1 s. 2 K scans were recorded with 32 dummy scans each. TOSCY and STD-TOCSY NMR spectra were recorded with 256 increments and 32 transients using a MLEV 17 spin-lock field of 60 ms at 7.5 kHz. The relaxation delay was set to 4 s.

### Ab initio MO calculations

The ab initio MO calculations were performed on SGI Octane and SGI Origin 2000 computers using the program GAUSSIAN 94. [16] Geometry optimization was carried out using HF/6-31G* [16] without restrictions. The chemical shifts subject to the ring current effect of aromatic/heteroaromatic ring moieties of amino acid residues of the enzyme were calculated based on the idea of NICS by Schleyer et al. [17] Accordingly, the molecule was placed in the center of a grid of ghost atoms ranging from –10.0 to +10.0 Å in all three dimensions with a step width of 0.5 Å, resulting in a cube of 68,921 ghost atoms. Because of the restrictions of GAUSSIAN 94 to 1,500 atoms, we had to split off the grid into 82 separate files. The chemical shielding calculations were processed with the GIAO method [18, 19] using HF/6-31G*. Since GIAO is a coupled HF method that uses gauge independent atom orbitals for the calculation of shielding values, it can be applied for the calculation of NICS.

From the results of the 82 GIAO calculations the coordinates and isotropic shielding values of the ghost atoms were extracted. After transformation of the tabulated chemical shieldings into a SYBYL [20] contour file, the ring current effect of the aromatic/heteroaromatic ring systems studied can be visualized as iso-chemical-shift surfaces (ICSSs). In this way is it possible to map the spatial extension, sign and scope of the ring current effect of the aromatic moieties studied. [21] In this paper, "fragmental ring current effects" of certain phenyl and heteroaromatic ring systems of the amino acid residues of hevamine in the binding site have been studied.

## Results

The naturally occurring chitinase inhibitor allosamidin was investigated by NMR spectroscopy in aqueous solution both in the free state and bound to hevamine. Concerning free allosamidin, we proved the conformational behavior of allosamidin in solution to be dominated by two to five preferred conformations with higher population in addition to many non-negligible conformers of lower population. In detail, we calculated six conformational families around the glycosidic linkage C1'–O–C4 and seven conformational families around the glycosidic linkage C1–O–C7. The experimentally obtained NOEs could only be matched if all of them were included into

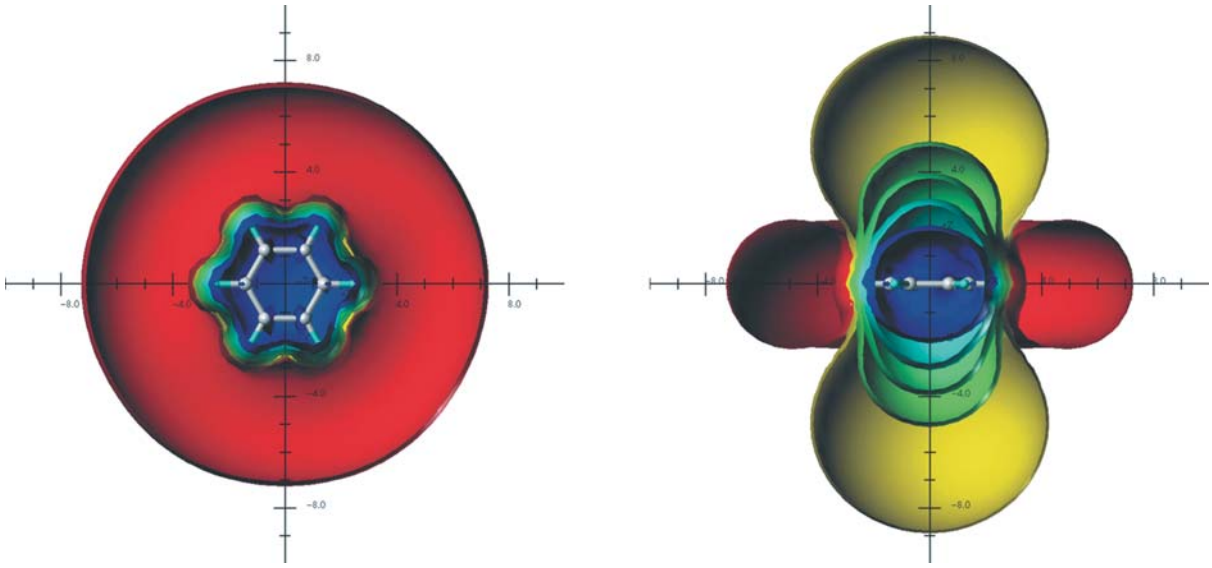

**Fig. 2** Calculated ring current effect of benzene (shielding ICSSs of –0.1 ppm, *yellow*, of –0.5 ppm, *green*, of –1 ppm, *green–blue*, of –2 ppm, *cyan* and of –5 ppm, *blue*, respectively; deshielding ICSS of +0.1 ppm, *red*) [14]

**Table 1** $^{1}$H and $^{13}$C chemical shift changes of allosamidin following the addition of hevamine

| Atom label | $^{1}$H δ (ppm) | $^{13}$C δ (ppm) |
|---|---|---|
| 7 | –0.13 | –0.2 |
| 8 | –0.28 | +1.8 |
| 9 | –0.25 | +5.1 |
| 10 | – | +1.7 |
| 11 | +0.42 | –0.5 |
| 12 | –0.19 | –0.4 |
| 13 | –0.03 | +0.4 |
| 14, 15 | –0.15 | –0.8 |

calculated population-weighted interglycosidic distances, leaving us with the information of a rather complex conformational behavior of allosamidin in the free state.

In order to study the conformation of allosamidin in complex with hevamine, the following NMR experiments were employed: HMQC, trNOESY, ROESY and STD NMR spectra. The trNOE experiment relies upon the fast exchange on the time scale of spin–lattice relaxation of free and bound ligand molecules. When a carbohydrate ligand is complexed with a large molecular weight protein, relaxation is determined by the protein's tumbling time, $\tau_c$, resulting in strong negative NOEs, so called trNOEs, that reflect the bound conformation. The STD technique is based on saturation transfer (by selectively irradiating the protein protons) from a protein to a ligand that binds to this protein through spin diffusion. Acquisition of on- and off-resonance spectra with subsequent subtraction generates difference spectra that contain only signals of ligand molecules that bind to the protein.

Actually, no STD and transfer NOE effects could be detected, although from a $K_i$ of 3.1 μM [9] positive answers could be expected. ROESY spectra alone are not able to distinguish between ROEs from free or bound states of the ligand. Therefore, it could only be concluded that, beside NOE zero crossing, increase of the pH during the NMR measurement, compared to the pH optimum of hevamine at pH=4, may be a reason for missing the transfer-NOE and STD signals.

On the other hand, the comparison of the HMQC spectra of both bound and free allosamidin showed significant signal shifts in the $^{1}$H and $^{13}$C dimensions of the allosamizoline part of the molecule (Table 1), indicative for the complex formation; chemical shift variations of other protons/carbons of allosamidin are negligible.

Only one set of signals for the bound allosamidin was observed and therefore the dissociation/association equilibrium proved to be fast on the NMR time scale. The general high field shift of the hydrogen atoms (except H-11) of the allosamizoline moiety could be a result of the hydrophobic contacts between this part of the inhibitor and the Trp255, Tyr183 and Tyr6 amino acid residues of hevamine (see later) which where found to be located in the binding pocket of hevamine in the X-ray structure.

In order to check whether the observed difference in the $^{1}$H chemical shift between free and bound allosamidin is caused by the influence of the ring current effect of Trp 255, Tyr183 and Tyr6 amino acid residues of hevamine, a more detailed ab initio MO study was carried out (see later).

Recently, Klod and Kleinpeter [21] reported the ab initio MO calculations of the anisotropic effect of a number of functional groups and the ring current effect of aromatic/heteroaromatic moieties. The intensity of the ring current effect proved to depend on both kind and number of condensed aromatic ring systems, which, due to the more delocalized π-electrons, extend the scope of the ring current effect. The ring current effects were visualized as ICSSs of identical values (e.g. the ring current effect of benzene in Fig. 2: the yellow shielding ICSS of –0.1 ppm at 9 Å from the center of the molecule). [21]

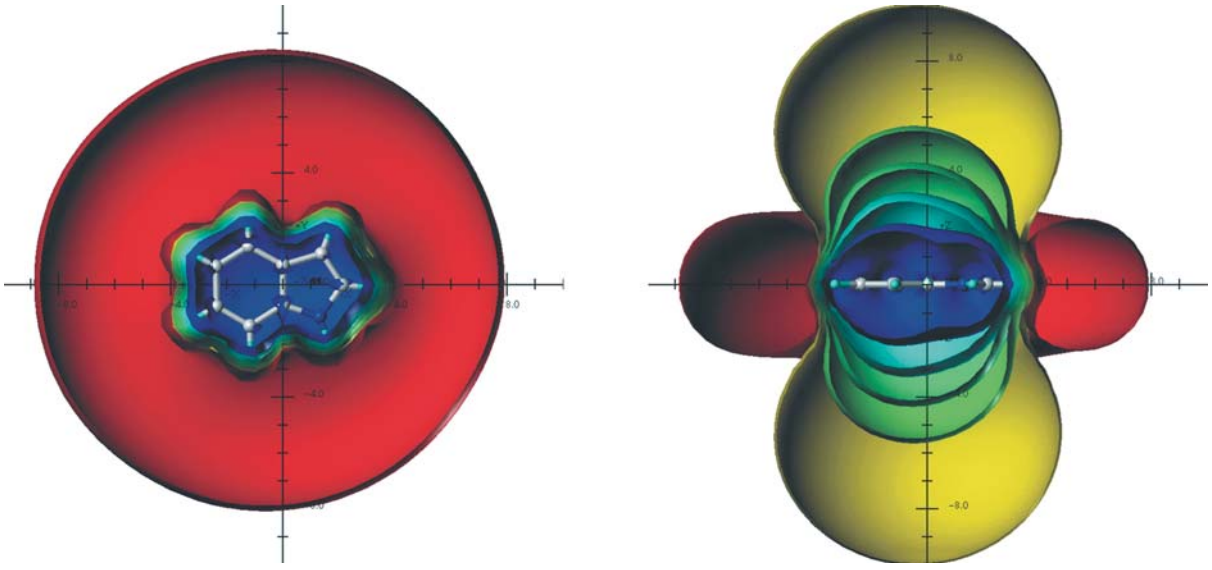

**Fig. 3** Calculated ring current effect of indole (shielding ICSSs of –0.1 ppm, *yellow*, of –0.5 ppm, *green*, of –1 ppm, *green–blue*, of –2 ppm, *cyan* and of –5 ppm, *blue*, respectively; deshielding ICSS of +0.1 ppm, *red*)

A similar ring current effect was calculated for pyrrole as a 5-membered heteroaromatic ring, [21] but less intense than in benzene; the deshielding ICSS of +0.1 ppm is observed at 6 Å in plane and the corresponding shielding ICSS of –0.1 ppm at 7.6 Å above and below the ring plane.

Employing this method, the ring current effect of the indole moiety of tryptophane was now calculated. From the former study, [21] we expected this condensed aromatic ring system to exhibit a stronger ring current effect than that obtained by simply combining the effects of the two original ring systems. Accordingly, the ring current effect of indole proved to be stronger; the shielding ICSS of –0.1 ppm reaches 10 Å above/below the ring plane and the deshielding ICSS of +0.1 ppm is obtained at 7.5 Å in the plane of the ring system. From these calculations it can be concluded that, from the tryptophane residues in protein structures, long range ring current effects can be expected (Fig. 3).

## Discussion

Terwisscha van Scheltinga et al. [7] studied the X-ray structure of the allosamidin–hevamine complex in the solid state. They found that in the crystal state (i) the allosamizoline moiety of allosamidin is bound at subsite –1, where the reaction intermediate is formed, and that (ii) the hydrophobic face stacks on the aromatic side chain of Trp255 while (iii) the two methyl groups make a strong van der Waals contact with the side chain of Tyr6. Furthermore, (iv) the allosamizoline group appears to be firmly fixed by hydrogen bonds. [7] This structural information is visualized in Fig. 1: beside allosamidin only those amino acid residues of the enzyme are given that are in close contact to the bound inhibitor. In the following, this crystal structure is compared with the chemical shift variations between free allosamidin and complexed to hevamine in aqueous solution (see later, Table 1). We were well aware that the solution structure of hevamine may differ from the X-ray structure. Nevertheless, due to the small temperature factors (*B* values) for each atom in the binding region, a conserved structure could be deduced. [7]

Due to significant complexation-induced chemical shift variations in the allosamizoline moiety of allosamidin (Table 1), it can be inferred that the van der Waals interactions between enzyme and inhibitor should be most active in this region; the substantial shift of H-11 (+0.42 ppm) of bound allosamidin to lower field in tandem with the shift of C-11 (–3.5 ppm) to higher field actually indicate high steric compression, which confirms that allosamidin is strongly in contact with hevamine in this position. The large low field shifts of C-9 (+5.1 ppm) and C-10 (+1.7 ppm), on the other hand, strongly indicate binding near to the strong proton acceptor groups Glu127 and Asp125, respectively, as found in the crystal structure and recent modeling studies. [7, 9, 10] Similarly, the C-8 and C-13 complexation-induced low field shifts of +1.8 ppm and +0.4 ppm, respectively, are in excellent agreement with existing hydrogen bonding between (OH)-8 and Gly81, and (OH)-13 and Ala224, respectively, as proposed by Terwisscha van Scheltinga et al. [7] in the crystal state.

Taking now further into account the ring current effects of indole and benzene moieties, the allosamidin bonding near to Trp255, Tyr6 and Tyr183 could also be analyzed quantitatively (Fig. 1). To begin with, the ring current effects of the corresponding indole and benzene moieties were calculated for the amino acid residues of hevamine close to the allosamidin complexation position (Fig. 1). Then, the chemical shifts of the protons of the allosamizoline moiety were analyzed with respect to

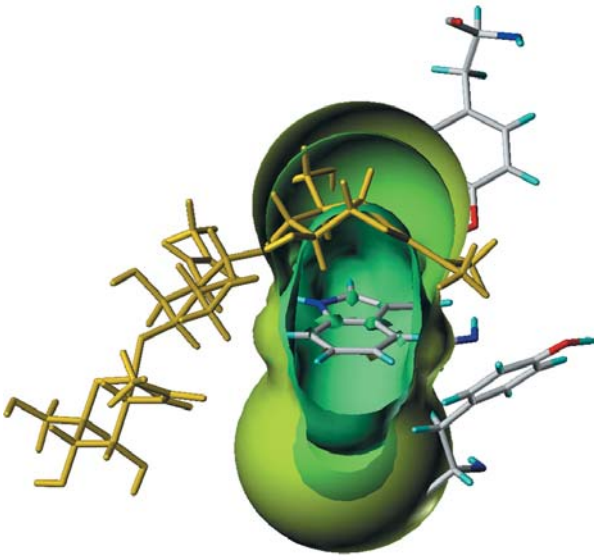

**Fig. 4** Calculated ring current effect of Trp255 (shielding ICSSs of –0.2 ppm, *yellow–green*, of –0.3 ppm, *light green* and –1 ppm, *green–blue*, respectively)

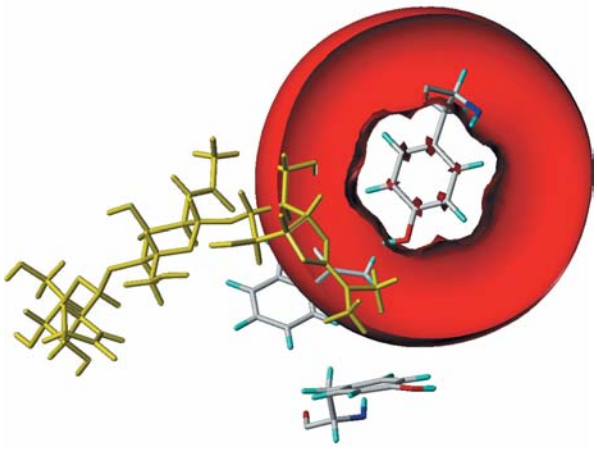

**Fig. 5** Calculated ring current effect of Tyr183 (deshielding surface of +0.1 ppm, *red*)

**Table 2** Experimental and calculated complexation-induced $^1$H chemical shifts

| | exp. Δδ ($^1$H) | calc. Δδ ($^1$H) |
|---|---|---|
| H-7 | –0.13 | –0.15 |
| H-8 | –0.28 | –0.5 |
| H-9 | –0.25 | –0.25 |
| H-11 | +0.42 | –0.20 |
| H-12 | –0.19 | –0.45 |
| H-13 | –0.03 | –0.05 |
| H-14, 15 | –0.15 | –0.2 |

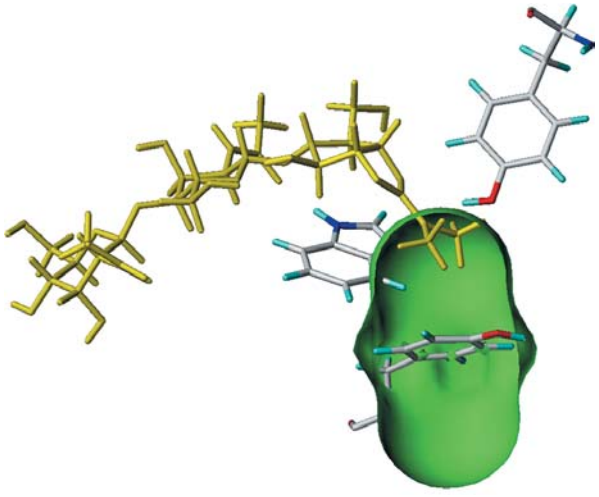

**Fig. 6** Calculated ring current effect of Tyr6 (shielding ICSS of –0.5 ppm, *cyan*)

both sign and intensity of the present ring current effect of these amino acids Trp255, Tyr6 and Tyr183. For reasons of clarity, the calculated ring current effects are discussed as isolated moieties and therefore, in a qualitative manner. The conclusions from the analysis were that the ring current effects in general could be influenced by the equilibrium between bound and free allosamidin, which is fast on the NMR time scale, but also by supplementary hydrogen bonding and electrostatic interactions to the amino acids and steric compression effects. As a qualitative measure, with respect to the fast exchange between free and bound allosamidin, the absolute shielding/deshielding ICSS values were bisected (these bisected values of the absolute values as calculated for the ring current effect together with the experimental values are compared in Table 2).

For the discussion of the respective influences on the proton chemical shifts in the allosamizoline moiety, only the shielding ICSSs are given for the amino acid residues of hevamine in Figs. 4, 5 and 6. For better understanding, portions of the ICSSs were cut in order to see the details.

The proton H-7 is localized on the –0.3 ppm shielding ICSS of Trp255 (Fig. 4). Because of the equilibrium between free and bound allosamidin, the absolute value was only considered as bisected, resulting in an overall shielding value of –0.15 ppm; compared to the experimental high field shift of –0.13 ppm, the agreement proves excellent both in sign and value. The corresponding position of H-7 with respect to Trp255 in the allosamidin complex in aqueous solution can be confirmed.

Like H-7, the protons H-8 and H-9 will also be shielded similarly by the ring current effect of Trp255, resulting especially for H-9 in an excellent agreement between calculated and experimental complexation-induced chemical shifts. In the case of H-8, the hydrogen is localized on the –1.0 ppm shielding surface of Trp255. The resulting bisected value of –0.5 ppm agrees with the experimental high field shift of –0.28 ppm in sign but not in amount; there is still a difference. We suspect that further influences, e.g. hydrogen bonding to (OH)-8 in solution, [7] could be the reason for the high field effect, which is lower than calculated.

For the proton H-11 a shielding of Δδ=–0.2 ppm has been calculated in the allosamidin–hevamine complex. This should result from the strong shielding of Trp255 (Δδ=–0.25 ppm) and a smaller deshielding of Tyr183 (Δδ=+0.05 ppm). However, the observed low field shift of +0.42 ppm cannot be the result of the ring current effect, but could, probably due to steric reasons, originate from the short distances to amino acid residues of the enzyme not considered in the present ab initio MO study. In such a case, electron density between hydrogen (H-11) and carbon (C-11) is shifted towards the carbon ($\Delta\delta_{C\text{-}11}$=–3.5 ppm) and away from the proton H-11 ($\Delta\delta_{H\text{-}11}$=+0.42 ppm) both in line with the experimental effects. [22]

The proton H-12 is localized on the –1.0 ppm shielding surface of Trp255 but the (bisected) shielding (Δδ=–0.5 ppm) is reduced by additional deshielding of Tyr183 (Δδ=+0.05 ppm) resulting in an absolute shielding of –0.45 ppm. Compared to the experimental value of –0.19 ppm, the calculated shielding of –0.45 ppm proves the stronger influence of Trp255 in contrast to the deshielding effect of Tyr183. In any case, it should be ascertained that the influence of the amino acids Trp255 and Tyr183 of hevamine is reflected correctly by the protons of the allosamizoline moiety, and $^1$H chemical shift variations prove this influence both in amount and sign. Small differences between the calculated values and the experiment can originate from small differences in crystal and solution structures of the hevamine–allosamidin complex.

The two methylene protons H-13a and H-13b are also shielded by Trp 255 but at the same time deshielded by Tyr183 (about the same amount); the agreement between calculated and experimental Δδ proves excellent. The two methyl groups C-14/C-15 are located on the +0.1 ppm deshielding surface of Tyr183. Because the internal rotation of the dimethylamino group is fast on the NMR time scale, a bisected deshielding of +0.05 ppm could be proposed for these dimethylamino protons. Further, they are rather shielded by Tyr6 (Δδ>–0.6 ppm). Thus, an overall shielding effect of Δδ=–0.2 ppm could be concluded, supporting both the excellent agreement between calculated and experimental values, and the assumption of the much stronger influence of Tyr6.

In summary, the calculated ring current effects of the aromatic moieties of Trp255, Tyr6 and Tyr183 of hevamine on the protons in the allosamizoline moiety of bound allosamidin strongly support a very similar structure of the hevamine–allosamidin complex both in solution and in the solid state.

## Conclusion

The influence of the ring current effects of Trp255, Tyr183 and Tyr6 moieties of hevamine on the $^1$H chemical shifts of the protons in the allosamizoline moiety of allosamidin in the allosamidin–hevamine complex resulting from binding to hevamine was calculated quantitatively by ab initio MO calculations; a theoretical model to quantitatively calculate the ring current effect of aromatic ring systems of the amino acid residues was employed. [21] By application of these ab initio MO calculations it was also possible to visualize the influence of the amino acid residues on the $^1$H chemical shifts of the protons in the allosamizoline region of allosamidin as ICSSs. The structure of the binding site in the allosamidin–hevamine complex appears to be very similar in solution and in the crystal state. Besides these hydrophobic contacts between allosamidin and hevamine, steric compression in the $^{13}$C NMR spectrum, charge polarization to the Glu127 amino acid residue of hevamine and hydrogen bonding to Try255 were also detected.

**Acknowledgements** AG thanks the Studienstiftung des deutschen Volkes for a scholarship.

## References

1. Ross AF (1961) Virology 14:329–339
2. Van Loon LC, Van Kammen A (1970) Virology 40:199–211
3. Fraser RSS (1981) Physiol Plant Pathol 19:69–76
4. Pierpoint WS (1986) Phytochemistry 25:1595–1601
5. Gianazzi S, Ahl P (1983) Neth J Plant Pathol 89:275–281
6. Archer BL (1976) Phytochemistry 15:297–300
7. Tervisscha van Scheltinga AC, Armand S, Kalk KH, Isogai A, Henrissat B, Dijkstra BW (1995) Biochem 34:15619–15623
8. Tervisscha van Scheltinga AC, Henning M, Dijkstra BW (1996) J Mol Biol 262:243–257
9. Brameld KA, Shrader WD, Imperiali B, Goddard WA (1998) J Mol Biol 280:913–923
10. Brameld KA, Goddard WA (1998) J Am Chem Soc 120:3571–3580
11. Sakuda S, Isogai A, Matsumo S, Suzuki A (1986) Streptomyces sp Tetrahedron Lett 27:2475–2478
12. Koga D, Isogai A, Sakuda S, Matsumo S, Suzuki A, Kimura S, Ide A (1987) Agric Biol Chem 51:471–476
13. Schlumbaum A, Mauch F, Vögeli U, Boller T (1986) Nature 324:365–367
14. Clore GM, Gronenborn AM (1982) J Magn Reson 48:402–417
15. Mayer M, Meyer B (1999) Angew Chem, Int Ed Engl 38:1784–1788
16. Frisch MJ, Trucks GW, Schlegel HB, Gill PMW, Johnson PG, Robb MA, Cheeseman JR, Keith T, Petersson GA, Montgomery JA, Raghavachari K, Al-Laham MA, Zakrzewski VG, Ortiz JV, Foresman JB, Cioslowski J, Stefanov BB, Nanayakkara A, Challacombe M, Peng CY, Ayala PY, Chen W, Wong MW, Andreas JL, Replogle ES, Gomperts R, Martin RL, Fox DJ, Binkley JS, Defrees DJ, Baker J, Stewart JP, Head-Gordon M, Gonzales C, Pople JA (1995) Gaussian 94, Revision E.2. Gaussian, Pittsburgh, Pa.
17. von Rague Schleyer P, Maerker C, Dransfeld A, Jiao H, van Eikema Hommes NJR (1996) J Am Chem Soc 118:6317–6318
18. Ditchfield JR (1974) Mol Phys 27:789–807
19. Cheeseman JP, Trucks GW, Keith TA, Frisch MJ (1996) J Chem Phys 104:5497–5509
20. SYBYL 6.6 (2000) Tripos Inc, St Louis MO 63144, S Hanley Road 303
21. Klod S, Kleinpeter E (2001) J Chem Soc, Perkin Trans 2 1893–1898
22. Pihlaja K, Kleinpeter E (1995) Carbon-13 NMR chemical shifts in structural and stereochemical analysis. In: Marchand AP (ed) Methods in Stereochemical Analysis. VCH, New York